論文 / 著書情報
Article / Book Information

Title	Correlations between aromaticity of dissolved organic matter and trace metal concentrations in natural and effluent waters: A case study in the Sagami River Basin, Japan
Authors	Tetsuro Kikuchi, Manabu Fujii, Koumei Terao, Jiwei Ran, Ying Ping Lee, Chihiro Yoshimura
Citation	Science of the Total Environment , Vol. 576, pp. 36-45
Pub. date	2017, 1
DOI	http://dx.doi.org/10.1016/j.scitotenv.2016.10.068
Creative Commons	See next page.
Note	This file is author (final) version.

License

Correlations between Aromaticity of Dissolved Organic Matter and Trace Metal Concentrations in Natural and Effluent Waters: A Case Study in the Sagami River Basin, Japan

Tetsuro Kikuchi[†], Manabu Fujii[†]*, Koumei Terao[†], Ran Jiwei[†],

Ying Ping Lee[†] and Chihiro Yoshimura[†]

[†] Department of Civil Engineering, Graduate School of Engineering, Tokyo Institute of Technology, 2-12-1-M1-4, Ookayama, Meguro-ku, Tokyo 152-8552, Japan

**Corresponding author: e-mail: fujii.m.ah@m.titech.ac.jp, Tel:+81-3-5734-2597*

Submitted to

Science of the Total Environment

2016

ABSTRACT

Chemical speciation, reactivity and bioavailability of trace metals in aqueous systems are strongly influenced by dissolved organic matter (DOM). DOM is a mixture of diverse components, so a range of organic molecules potentially participates in the occurrence of dissolved trace metals. In this study, we investigated water quality variables that influence dissolved trace metal concentrations in natural and effluent water systems with a particular attention given to the relationship between DOM optical properties and dissolved copper and iron concentrations. We found that specific UV absorbance ($SUVA_{254}$: an indicator of DOM aromaticity) has a significant correlation with dissolved trace metal to dissolved organic carbon concentration ratios ($[Me]_T/[DOC]$) for copper and iron in natural freshwaters and treated municipal wastewater in the Sagami River basin, Japan. This trend was also prevalent for other freshwaters in temperate climates except for Fe-rich waters. Our findings indicate that the concentrations of dissolved copper and iron in natural and effluent waters are significantly influenced not only by DOM concentration but also by aromaticity of DOM, and that this DOM property can be inferred from spectrophotometric measurements.

1. Introduction

Dissolved organic matter (DOM) in aqueous systems has several environmental and ecological functions, including acting as a proton and metal ion buffer (Ritchie and Perdue, 2003; Tipping, 2002), participating in redox reactions (Fimmen et al., 2007), absorbing solar light (Morris et al., 1995), and providing a source of nutrients and energy (Keil and Kirchman, 1991; Wetzel, 1992). DOM consists of a range of organic molecules, of which humic substances (HS) are the primary metal-binding ligands for trace metals including copper (Cu) and iron (Fe) (Tipping, 2002). Other biogenic ligands, such as amino acids and saccharides, also significantly contribute to metal complexation in some circumstances (Croue et al., 2003; Hassler et al., 2011). Although most metal-binding ligands comprise oxygen (O)-containing acid functional groups such as carboxyls and phenols (Tipping, 2002), relatively low abundance nitrogen (N)- and sulfur (S)-containing functional groups display strong binding affinities for trace metals (Craven et al., 2012; Croue et al., 2003; Frenkel et al., 2000; Laglera and van den Berg, 2003; Smith et al., 2002). Other factors including local molecular structure (e.g., in proximity to metal-binding sites) may be significant in metal coordination by DOM (Fujii et al., 2014; Hertkorn et al., 2006; Karlsson et al., 2006). These findings highlight the importance of the DOM molecular information in understanding of DOM-metal interactions.

Advanced techniques such as X-ray absorption spectroscopy enable researchers to investigate DOM-metal coordination at the atomic and molecular level (Frenkel et al., 2000; Karlsson and Persson, 2010; Karlsson et al., 2006; Karlsson and Skyllberg, 2007; Vachet and

Callaway, 2003), but classical spectrophotometric techniques, including UV-Vis absorbance and fluorescence, are also widely used to characterize DOM and its interaction with metals. Techniques for measuring absorbance and fluorescence are relatively rapid, simple, and inexpensive. Importantly, these techniques do not require multi-step pretreatment, which can result in the isolation of specific fractions or alternation of the original DOM composition. Although such spectrophotometric measurements can only detect specific moieties in DOM, including conjugated structures (e.g., partially oxidized lignins) (Boyle et al., 2009), DOM optical indices are nonetheless expected to be useful descriptors of metal-binding by DOM in aquatic environments as noted below.

A previous study on the copper (Cu), zinc (Zn), cadmium (Cd), and nickel (Ni) complexation with freshwater DOM isolated using reverse osmosis indicated that the specific UV absorbance ($SUVA_{254}$: ratio of absorbance at a wavelength of 254 nm [A_{254}] relative to the dissolved organic carbon [DOC] concentration) has a significant positive correlation with the metal binding affinity (a parameter defined by the concentration ratio of DOM-bound metal relative to DOC) (Baken et al., 2011). Similar correlations between $SUVA_{254}$ and the capacity of 15 types of humic acids (HA) and fulvic acids (FA) to complex ferric iron (Fe[III]) (Fujii et al., 2014), and between $SUVA_{254}$ and the Cu binding affinity of dissolved soil organic matter (Amery et al., 2007), have also been recognized. Given that $SUVA_{254}$ correlates well with the aromatic characteristics of DOM, including aromaticity (Weishaar et al., 2003), and that a study of 30 U.S. rivers showed a strong correlation between $SUVA_{254}$ and the proportion of hydrophobic fraction in DOM (Spencer et al., 2012), these previous findings suggest that transition metals such as Fe and Cu may be preferentially complexed by DOM aromatic moieties with high $SUVA_{254}$ in aqueous systems. A further evidence of Cu complexation by aromatic compounds (such as photochemically-derived humic acids from tyrosine) has been recently indicated by Berto et al. (2016). Besides $SUVA_{254}$, the differential absorbance and slope of normal (or log-transformed) absorbance spectrum for Suwannee River DOM have been found to be correlated with concentrations of metals bound to DOM in the pH range from 5 to 11 (e.g., Cu, Fe, calcium [Ca] and magnesium [Mg]). These facts generally suggest that metal complexation by DOM is accompanied by the replacement of protons in carboxylic and phenolic functional groups, though the direct measurement using advanced techniques may be required to understand the detailed complexation mechanism (Gao et al., 2015; Yan and Korshin, 2014, Yan et al., 2013a, 2013b, 2013c; Yan et al. 2015). However, previous studies were conducted using operationally isolated DOM and concentrations of DOM and metals higher than those typically found in the natural environment, and therefore may not directly demonstrate the applicability of DOM optical parameters for predicting concentrations of dissolved trace metal complexes in environmental water systems exhibiting a range of water qualities. For example, the concentrations of DOC and trace metals used in the laboratory experiments of two comparative studies (Baken et al., 2011; Fujii et al., 2014) is a few orders of magnitude higher than those found in the natural and effluent waters including the observation in the present study (see Supporting Material [SM] Table S1). In addition, it has been reported that optical indices of DOM can be in some cases affected by solution chemistry such as pH and concentrations of Ca ion and DOM (Yang and Hur, 2014).

This study aimed at analyzing the capability of DOM optical indices to predict concentrations of dissolved trace metals in natural freshwaters (river and reservoir waters) and effluents discharged from municipal wastewater treatment plants (WWTP) in the Sagami River Basin (SRB), Japan and other freshwater systems in temperate and other climates. In this study, the spatiotemporal characteristics of water quality variables in the SRB were firstly investigated followed by the examination of specific relationships between DOM optical indices and the trace metal related parameters including metal-to-DOC concentration ratios ($[\mathrm{Me}]_T/[\mathrm{DOC}]$, where $[\mathrm{Me}]_T$ is the total dissolved concentration of Cu, Fe, or Zn) (see SM Section S1 for further detailed definitions and characteristics of the optical indices and other parameters used in this study). The DOM optical indices include SUVA_{254}, spectral slope in the wavelength region 275–295 nm [$S_{275\text{-}295}$] (Helms et al., 2008), and fluorescence index [FI] (McKnight et al., 2001); these indices represent DOM aromaticity, average molecular weight, and source, respectively.

2. Materials and Methods

2.1 General

A full description of the materials and methods is found in Section S2, which includes characteristics of study area, field survey, chemical analysis and measurement, quality control in the trace metal determination, UV absorbance correction and analysis using literature data. The calculation of trace metal speciation is also provided in Sections 2.4 and S3.

2.2 Study area and chemical analysis

Surface water samples were collected from the fixed sampling stations in the Sagami River basin (SRB) in Japan. The characteristics of this river basin and sampling stations are detailed in Sections S2.1 and S2.2. Water quality parameters, including the concentrations of dissolved organic carbon and trace metals, absorbance and fluorescence spectra, inorganic nutrients, water temperature, pH, and electrical conductivity, were measured according to the procedures described in Section S2.3.

Briefly, the water samples were filtered through an acid-washed polytetrafluoroethylene (PTFE) membrane filter with 0.45 μm pore size (Omnipore JHWP, Merck Millipore, Billerica, MA). The concentration of DOC ([DOC]) was determined as non-purgeable organic carbon (NPOC) using a TOC analyzer (TOC-5000, Shimadzu, Kyoto, Japan). Absorbance spectra were measured using a UV-visible spectrophotometer (UV-1800, Shimadzu) with a 1-cm path-length quartz cuvette. Since the measured absorbance for our SRB water samples (e.g., $>6.43 \times 10^{-3}$ cm^{-1}) was sufficiently higher than the analytical detection limit of spectrophotometer used (1.5×10^{-4} cm^{-1} calculated by assuming 3-fold of the background noise level; see Section S2.3), a 1-cm pathlength cuvette was selected for the absorbance measurement. Specific UV absorbance at a wavelength of 254 nm ($SUVA_{254}$) was calculated as the baseline-corrected absorbance at 254 nm (A_{254}) relative to [DOC] (Weishaar et al., 2003). Spectral slope in the wavelength region 275–295 nm ($S_{275\text{-}295}$) was determined by applying linear regression to natural log-transformed absorbance data in the corresponding wavelength region (Helms et al., 2008). It is widely recognized that dissolved forms of Fe and nitrate absorb UV light and therefore potentially interfere with DOM absorbance measurements in the UV region (Buck et al., 1954; Poulin et al., 2014; Weishaar et al., 2003). As described in Section S2.4, however, the contributions of Fe and nitrate in SUVA_{254} measurement were generally determined to be small. Note that all A_{254} and SUVA_{254} values presented in this study were corrected for the concentrations of dissolved Fe and nitrate where these data were available. Fluorescence index (the ratio of emission intensities at 450 nm relative to 500 nm with excitation at 370 nm) were determined using a spectrofluorophotometer (RF-5300PC, Shimadzu) (McKnight et al., 2001). Yang and Hur (2014) indicated that FI value for the solution containing ~10 mg-C.L^{-1} DOM decreases by a 0-0.5 unit after the 10-folds dilution. Although [DOC] of the SRB effluents was higher than that of the natural waters by 5 folds (Table 1), any corrections were not performed in the determination of FI for both of the natural and effluent waters, because no systematic trends between FI an [DOC] have been retrieved in this study (e.g., Yang and Hur, 2014). Ultrapure water (Milli-Q water, ~2 ppb total organic carbon level, 18.2 MΩ·cm resistivity at 25°C, Merck Millipore) was used as a blank in the absorbance and fluorescence analyses.

For determination of total dissolved major and trace elements, a portion of the filtered sample was acidified by adding concentrated nitric acid (reagent grade, Kanto Chemical, Tokyo, Japan) at a final concentration of about 2% (v/v) (ca. 0.3 M) and the concentrations of total dissolved trace metals (Cu, Fe, and Zn) and major elements (Ca, Mg, and silica [Si]) were determined using an inductively coupled plasma mass spectrometer (ICP-MS; 7700x, Agilent Technologies, Santa Clara, CA). The detection limit of each element in the ICP-MS analyses is summarized in Table S2. Metal concentrations in the certified reference material (CRM) for river water (CRM 7202-b, National Metrology Institute of Japan, National Institute of Advanced Industrial Science and Technology) were also measured using an identical procedure to those employed for the SRB water samples. Measured recoveries for the metals in this CRM ranged from 89% for Zn to 103% for Mg (Table S3), ensuring a sufficiently high accuracy of analysis. Further considerations in Fe measurement are provided in Section S2.5.

2.3 Literature data

To assess the generality of our results, the SRB data were compared with the literature. Data from four natural freshwater systems were used to analyze $[\mathrm{Me}]_T/[\mathrm{DOC}]$ (Me: Cu, Fe and Zn) and DOM optical indices: (i) the Hwangryong River watershed, Korea (HRW) (Park et al., 2007), (ii) the Yukon River basin, Alaska (YRB) (Stolpe et al., 2013) and (iii) freshwaters in Belgium and Germany (BGF) (Baken et al., 2011). Information on DOM optical indices, [DOC] and $[\mathrm{Me}]_T$, as well as the climatic and geological settings for the SRB and other systems are summarized in Table 1. For BGF waters only, the concentration of DOM-bound metal ([MeL]) has been reported (Baken et al., 2011).

However, the BGF data (i.e., [MeL]) were treated as $[Me]_T$ in an identical manner to those for the other regions by assuming that [MeL] is equivalent to $[Me]_T$, since the DOM-bound form (MeL) was determined to account for a majority of total dissolved metal in the BGF waters (e.g., on average >99% for Cu) (Baken et al., 2011). To our knowledge, only these three previous studies provided datasets appropriate for comparative analysis.

2.4 Model calculation

Speciation of dissolved trace metals in SRB waters, including the DOM-bound form, was predicted using the chemical equilibrium calculation software Visual-MINTEQ coupled with the Non-Ideal Competitive Adsorption (NICA)-Donnan model (hereafter referred to as “VMIN-ND”). Detailed calculation methods (e.g., input data sets and condition settings) and associated results and discussion are summarized in Section S3. Briefly, the water quality parameters measured in SRB were directly used as input data to the model, except for pH and EC which were input after conversion into log-transformed activity of proton (H^+) and ionic strength (I). The fraction of HS in DOM (f_{HS}) was taken as 0.35 and 0.25 for natural waters and WWTP effluents, respectively, according to previous reports in Japan (Imai et al., 2001; Imai et al., 2002). For the fraction of FA in HS (f_{FA}), 0.35, 0.55, and 0.75 were used in the SRB natural waters (where average [DOC] was 1.0 mg L^{-1}) and a fixed value (0.75) was used for the WWTP effluents (where average [DOC] was 5.5

mg L^{-1}), according to the reported f_{FA} : [DOC] ratio in previous studies for a range of natural waters (Nagao, 2008).

2.5 Statistical analysis

Single correlation coefficients between couples of parameters were determined. Normal distributions for the set of parameters were tested by the Kolmogorov-Smirnov test prior to correlation analysis. If the normality of both parameters of interest was confirmed, Pearson's correlation coefficient (r) was calculated; otherwise, Spearman's rank correlation coefficient (r_s) was applied (Quinn and Keough, 2002). Principal component analysis (PCA) was also performed to assess the interaction among the measured parameters. Each parameter was scaled by its standard deviation in order to weigh the contribution of each parameter to the principal components equally (Bundy et al., 2014). All measured parameters in this study were well above the detection limit (DL) except for $[Fe]_T$, A_{254}, and some inorganic nutrients, as noted in Section S2.7. The data below DL (BDL) for these parameters were excluded from the statistical analyses (and speciation calculation by VMIN-ND). However, the correlation coefficients determined under this condition were almost identical to those calculated under the assumption that the measured BDL data is either null or a half value of DL. All the statistical calculations were performed with the statistical software R.

3. Results and Discussion

3.1 Spatiotemporal characteristics of water quality variables in the Sagami River Basin (SRB)

All water quality parameters measured in this study are listed in Table S4 and summarized in Table 1. To investigate the interaction among water quality parameters and their spatiotemporal trends, PCA analyses were performed for the water quality data from the SRB natural waters (Figure 1a and 1c) and all SRB waters including natural waters and WWTP effluents (Figure 1b and 1d).

In the SRB natural waters, the first principal component (PC1) accounted for 26% of total variance in the dataset examined with this component being dominated by the loadings from major cations (e.g., Ca and Mg) and nutrients (e.g., nitrate and Si) (Figure 1a). The second principal component (PC2) explained 20% of total variance and this component was characterized by the loadings from dissolved oxygen and DOM optical properties including $SUVA_{254}$ and FI (Figure 1a). Other parameters such as water temperature, [DOC], and total concentration of dissolved trace metals ($[Cu]_T$ and $[Fe]_T$) were also associated with PC2, although their loadings were negative. As can be seen in Figure 1c, the sampling sites in the main stream including two reservoirs had relatively higher scores for PC1 compared to those in the tributaries. This result is basically consistent with the fact that the SRB main stream waters contained higher concentrations of major cations and nutrients than those for tributaries (Table 1), as the main stream is affected by the pollution load from the urbanized catchment including domestic, agricultural, and industrial activities (see Table S5 for pollution load data).

Regarding the temporal characteristics, the score for PC2 was higher in winter and lower in summer for both main stream and tributaries (Figure 1c). This result combined with the significant loading of water temperature to PC2 (Figure 1a) suggests that the score for PC2 represents seasonal variation. Given that [DOC] and DOM optical properties (e.g., $SUVA_{254}$ and FI) had significant loadings to PC2, it is likely that these DOM-related parameters also vary seasonally (see Section 3.5 for the detailed discussion). This is also consistent with the trend typically observed in natural waters where [DOC] is higher in summer due to production of autochthonous organic matters from growth (and cell lysis) of microorganisms including algae. In addition, the observed lower concentrations of nitrate and divalent cations (Ca and Mg) in summer are likely reasonable given the higher nutrient consumption by microorganisms in this season and precipitation of carbonate salts in warmer water (Table S4). The PCA results for all SRB waters including natural and WWTP-treated waters (Figure 1b and d) indicated that PC1 and PC2 account for 51% and 14% of total variance, respectively and PC1 is characterized by high concentrations of major and trace metals as well as high [DOC] and A_{254}. Given the relatively high concentrations of these water quality parameters in the WWTP effluent, it is reasonable that PC1 is associated with WWTP effluents (Figure 1d and Table 1).

3.2 Relationship between DOM optical parameters and trace metal related parameters in SRB

In Table 2, single correlation coefficients between total dissolved metal ($[Me]_T$) and other water quality parameters are summarized. For the main stream, $[Cu]_T$ and $[Fe]_T$ had significant positive correlations with [DOC] and water temperature ($p < 0.001$). In addition, $[Cu]_T$ and $[Fe]_T$

were also positively correlated with each other ($p < 0.001$). Concentration of Zn showed different correlation pattern from the other two metals (e.g., significant negative correlation with water temperature [$p < 0.001$]). Relatively weak ($p < 0.05$) or insignificant ($p > 0.05$) correlations were found between $[Me]_T$ and DOM optical indices for all metals. In the tributaries, there were no significant correlations between [DOC] and $[Me]_T$. In contrast, $[Cu]_T$ and $[Fe]_T$ were still positively correlated with each other ($p < 0.001$) and this trend was similar to the main stream. In the tributaries, correlations between $[Me]_T$ and DOM optical parameters were also relatively weak ($p < 0.05$) or insignificant ($p > 0.05$). In the WWTP effluents, correlations between $[Me]_T$ and water qualities were less clear and their trends were different from those observed in the natural waters. It should be noted that the result of correlation analysis for the log-transformed data (Table S6) was almost identical to that for the normal data (Table 2).

When the majority of dissolved metal occurs in DOM-metal complex form, the metal-to-DOC concentration ratio (e.g., $[Me]_T/[DOC]$) is approximated to be equal to the amount of bound metal per unit carbon mass of DOM (i.e., [MeL]/[DOC]). Indeed, the model calculation using VMIN-ND indicated that MeL accounted for 99 ± 3% and 88 ± 11% (average ± standard deviation) of total dissolved Cu and 99 ± 7% and >99.9% of total dissolved Fe in the SRB natural waters (n = 90) and effluents (n = 6), respectively, while inorganic species accounted for on average 59% and 96% of the total dissolved Zn in the natural and effluent waters, respectively (Table S7). Therefore, we considered that the comparison of $[Me]_T/[DOC]$ with DOM-related parameters is a reasonable approach at least for the case of Cu and Fe. The correlation analyses between $[\mathrm{Me}]_T/[\mathrm{DOC}]$ and water quality parameters including DOM optical indices were performed for the SRB natural and WWTP effluent waters. As can be seen in Table 3, significant positive correlations were observed between SUVA_{254} and $[\mathrm{Me}]_T/[\mathrm{DOC}]$ for all metals in the natural waters ($p < 0.01$). In particular, strong linear correlations were found between SUVA_{254} and $[\mathrm{Cu}]_T/[\mathrm{DOC}]$ with the correlation coefficients (r) of 0.68 and 0.69 for the main stream and tributaries, respectively (Figure 3a and Table 3). Although the correlations between SUVA_{254} and $[\mathrm{Me}]_T/[\mathrm{DOC}]$ for Fe and Zn were relatively weak overall, there were still significant linear correlations in the tributaries ($r = 0.72$ for Fe and $r = 0.64$ for Zn, Figure 3b, c and Table 3). The results of PCA with respect to $[\mathrm{Me}]_T/[\mathrm{DOC}]$ and other parameters also supported the correlation for SUVA_{254} and $[\mathrm{Cu}]_T/[\mathrm{DOC}]$ (Figure 2). For example, in the PCA for all SRB waters, both SUVA_{254} and $[\mathrm{Cu}]_T/[\mathrm{DOC}]$ had significant loadings to PC2 whereas the loadings of these parameters to PC1 were relatively small (Figure 2b). For the other DOM optical indices ($S_{275\text{-}295}$ and FI), no systematic trends were retrieved in terms of correlation with $[\mathrm{Me}]_T/[\mathrm{DOC}]$ (Table 3), implying that variation of $[\mathrm{Me}]_T/[\mathrm{DOC}]$ is not necessarily explained by DOM molecular weight (i.e., $S_{275\text{-}295}$) or source (i.e., FI; e.g., terrestrial and microbial origin).

It is well recognized that pH is one of the important factors that substantially influence trace metal complexation by DOM, as pH affects metal and DOM chemistry including metal hydrolysis and protonation/deprotonation of the metal-binding ligands in DOM. However, in the SRB natural waters, $[\mathrm{Me}]_T/[\mathrm{DOC}]$ for all metals had no significant correlations with pH except for the case of Cu in the tributaries (negative correlation between pH and $[Cu]_T/[DOC]$ with $p < 0.01$) (Table 3). For Cu, our calculation using VMIN-ND indicated that the fraction of Cu bound to DOM (i.e., $[CuL]/[Cu]_T$) in the SRB natural waters slightly decreases only at the lower pH values (e.g., <7.5) (Figure S1a). The calculation also indicated the negative relationship between $[CuL]/[Cu]_T$ and $[Cu]_T/[DOC]$ (Figure S2a). While these calculations generally suggest that $[Cu]_T/[DOC]$ is higher at lower pH, the samples with pH <7.5 accounted for only 15% of the SRB natural waters (Table S4). Therefore, the plausible reasons for the weak correlation between $[Cu]_T/[DOC]$ and pH are that (i) the majority of water samples examined had relatively high pH (e.g., >7.5), (ii) most of dissolved Cu was in the form of Cu-DOM complex at the higher pH values, and thus (iii) the effect of pH on Cu speciation was relatively small in our sample set. For Fe and Zn, the decreasing trend of $[MeL]/[Me]_T$ with decreasing pH were also indiscernible as shown in Figure S1b and c, although a weak positive relation was observed for Zn due possibly to (i) the significant competition of Zn complexation by DOM with proton at lower pH and (ii) a weaker binding affinity of Zn for DOM complexation.

3.3 Comparison with other natural water systems

To assess the generality of the observed relationships, identical analyses were conducted following incorporation of previously reported data from other natural waters (Baken et al., 2011; Mueller et al, 2012; Park et al., 2007; Stolpe et al., 2013) (Table 1). Consequently, the data for Cu and Fe in HRW and BGF fell well within the range of variation in SRB waters. This is demonstrated in Figure 3, which depicts scatter plots of $SUVA_{254}$ versus $[Me]_T/[DOC]$. In particular, the linear regression line for [CuL]/[DOC] and $SUVA_{254}$ in the BGF waters which receive no urban effluents was comparable to that observed for $[Cu]_T$/[DOC] in the SRB tributaries (which are also less affected by the anthropogenic discharges; Figure 3a).

However, in some waters, $[Cu]_T$/[DOC] and $[Zn]_T$/[DOC] were substantially lower or varied in the similar level of $SUVA_{254}$. For example, in YRB waters, $[Cu]_T$/[DOC] and $[Zn]_T$/[DOC] were observed to be lower than those for SRB and HRW waters, when compared at the same level of $SUVA_{254}$ (Figure 3a and c). Similarly, for the DOM isolates in acidic BGF waters, relatively lower [CuL]/[DOC] and [ZnL]/[DOC] values were observed at the same $SUVA_{254}$ level. In these waters, high concentrations of dissolved Fe were observed (e.g., 2.4–17 μM for YRB [Stolpe et al., 2013]; >10 μM for acidic BGF waters [Baken et al., 2011], Table 1). Plausible explanations for the relatively lower $[Cu]_T$/[DOC] and $[Zn]_T$/[DOC] in the Fe-rich waters are due to (i) competing effect of Fe on the complexation of Cu or Zn by DOM and (ii) scavenging of dissolved Cu or Zn by Fe-rich particulates. Regarding the first case, for example, equilibrium calculation by Tipping et al. (2002) indicated that Fe(III) significantly competes with Cu and Zn for complexation by DOM over a wide pH range (4–9). Consistently, an additional analysis using our data set showed that $[Zn]_T$/[DOC] in SRB and HRW waters tends to increase as $[Zn]_T/[Fe]_T$ increases at the same $SUVA_{254}$ level (Figure S7b). Thus, the binding of Cu and Zn (especially the latter metal) by DOM are at least partially hindered by the competition with Fe for complexation by DOM, resulting in lower $[Me]_T$/[DOC] values at the same $SUVA_{254}$. For the second case, laboratory-based studies have shown that Cu and

Zn can be scavenged by Fe oxyhydroxide colloids via adsorption, surface precipitation and/or co-precipitation with Fe depending on the metal-to-Fe molar ratio (Karthikeyan et al., 1999; Trivedi et al., 2004). The aggregation of Fe(III) oxyhydroxide particles may retard desorption of Cu ion incorporated in the aggregate due to physical constraint (Gilbert et al., 2009).

3.4 Effects of effluent-derived components

The SRB tributaries and BGF waters with less anthropogenic impacts showed $[Cu]_T/[DOC]$ lower than those for the SRB main stream and BGF waters with urban inputs, when compared at the same $SUVA_{254}$ level (Figure 3a). This may suggest that the increasing $[Cu]_T/[DOC]$ value in anthropogenically-impacted SRB and BGF waters is attributed to the anthropogenic components including metal-binding ligands with low $SUVA_{254}$ and relatively high complexation affinity in addition to high Cu concentration in the effluent. Regarding the metal-binding ligands, for example, Baken et al. (2011) suggested that aminopolycarboxylate ligands (mainly ethylenediaminetetraacetic acid [EDTA]) were detected at concentrations of 4.8–140 nM in the anthropogenically-influenced BGF waters (Table 1) and partially explained the relatively higher [CuL]/[DOC]. Although concentrations of anthropogenic metal-binding ligands including EDTA are not reported for the WWTP effluents in the SRB, the concentration of WWTP-derived EDTA in the SRB main stream was roughly estimated to be 0.08–38 nM by using the literature data (see Section S2.8 for the detailed calculation). In addition, given that $SUVA_{254}$ for EDTA is negligibly small (e.g., ~0.06 L

mgC^{-1} m^{-1} according to the measurement of EDTA absorbance spectrum), it is unlikely that EDTA present in natural waters substantially accounts for $SUVA_{254}$. Therefore, the WWTP-derived metal-binding ligands with low $SUVA_{254}$ may also occur in the SRB main stream to some extent and potentially increase $[Cu]_T/[DOC]$ in the anthropogenically-impacted waters, compared to less impacted waters at equal $SUVA_{254}$.

However, according to the aforementioned PCA for all SRB waters (i.e., natural waters and WWTP effluents), [DOC], A_{254} and $[Cu]_T$ had high loadings to PC1 and these parameters also showed the divergent trends from $SUVA_{254}$ and $[Cu]_T/[DOC]$ (Figures 1b and 2b). This result, therefore, indicates that the observed correlation for $SUVA_{254}$ and $[Cu]_T/[DOC]$ in the anthropogenically-influenced SRB main stream could not be described simply by mixing process of WWTP effluents characterized by high [DOC], A_{254} and $[Cu]_T$ with river waters which generally have low [DOC], A_{254} and $[Cu]_T$ (Table 1 and Figures 1d and 2d). Thus, our data generally suggest that the relatively large variation for $[Cu]_T/[DOC]$ in the SRB main stream cannot be solely explained by the influences of anthropogenic metal-binding ligands and Cu discharged from WWTP. Other plausible reasons for the observed variation of $[Cu]_T/[DOC]$ may include the inputs from other types of urban discharge with different water quality and non-point sources (e.g., livestock, agriculture, industrial sectors, etc. as shown Table S5). In addition to the anthropogenic ligands, hydrophilic DOM fraction and dissolved sulfides originated from urban effluents may affect trace metal speciation due to their high binding affinities to trace metals (Chaminda et al., 2013; Louis et al., 2014; Matar et al., 2015; Rozan et al., 2000).

3.5 Seasonal characteristics

The PCA analyses underlined the seasonal variation of DOM optical properties (e.g., $SUVA_{254}$ and FI). Indeed, lower $SUVA_{254}$ values (i.e., DOM aromaticity) were observed for the SRB natural waters during the high irradiance season (i.e., summer) ($p < 0.05$ according to the pairwise t test by Holm’s method, Table S8 and Figure S3). Previous laboratory-based experiments also demonstrated a significant reduction in $SUVA_{254}$ for freshwater DOM following irradiation with a solar simulator (Brooks et al. 2007). These results may suggest that a higher degree of photochemical degradation of colored dissolved organic matter (CDOM) is associated with a decrease in DOM aromaticity, which in turn results in a decreasing metal-to-DOC ratio. A previous study by van den Berg et al. (1987) reported that the total dissolved Cu concentration ($[Cu]_T$) in water from the Scheldt estuary in the Netherlands co-varied with the concentration of strong Cu-binding ligand. In addition, total dissolved Fe concentration ($[Fe]_T$) was maintained at levels just below the Fe-binding capacity of HS in other coastal waters (Thurso Bay and the Irish Sea, U.K.) (Batchelli et al. 2010, Laglera and van den Berg 2009). Therefore, it is interesting to investigate the seasonal variation of metal binding characteristics (e.g., stability constant and complexation capacity) and the relations to DOM aromaticity and metal speciation in future study.

4. Conclusions

Previous studies indicated that [DOC] is an important factor that influences solid/solution partitioning and spatiotemporal variation of dissolved trace metals (e.g., Cu, Zn, and Cd) in natural aqueous systems. However, in some cases, [DOC] is not the best predictor of these metal concentrations (Lu and Allen, 2001; Shafer et al., 1997). By examining the correlation of DOM optical indices and trace metal related parameters in natural freshwaters and WWTP effluents, our study indicated that the metal-to-DOC concentration ratios for Cu and Fe (which exhibit higher affinities for DOM compared to Zn) are highly associated with the optical properties of DOM in the Sagami River basin and other freshwaters in temperate climates except for Fe-rich waters. The observed correlation for metal-to-DOC ratio and $SUVA_{254}$ indicates that aromaticity is an important DOM qualitative factor that determines the concentrations of trace metal complexes in natural and effluent waters. Indeed, the Fe(III) and Cu(II) complexation capacities of natural organic matters (e.g., 15 species of standard humic substances (Fujii et al., 2014) and soil organic matters (Amery et al., 2007)) are positively correlated with their aromaticity (i.e., $SUVA_{254}$). The findings suggest that these trace metals are preferentially complexed by the metal binding ligands (e.g., acidic functional groups) resident in the proximity of aromatic structures of humic materials.

Overall, our findings generally indicate that the concentrations of these dissolved trace metals in natural freshwater systems (e.g., rivers and reservoirs) and wastewater effluents are regulated not only by the concentration of DOM but also by its molecular properties that can be estimated by simple optical measurements. Hence, the assessment of DOM optical properties may be useful to understand the trace metal-DOM interaction and metal bioavailability in natural and effluent water systems.

ACKNOWLEDGEMENTS

We appreciate the financial supports from JST CREST, JSPS Young Scientists (A) (25709045) and the Bilateral Joint Research Project. The financial support from the Ministry of Environment – Japan (Environment Research and Technology Development Fund S-13-2-3) is also appreciated.

AUTHOR CONTRIBUTIONS

T. K., M. F., K.T. and J.R. performed the field survey. T. K., K.T. and J.R. performed the experiments. T. K., M.F., Y.P.L. and C.Y. analyzed and interpreted the data. T. K., M.F., Y.P.L. and C.Y. drafted the manuscript. All authors reviewed the manuscript.

SUPPLEMENTARY MATERIAL

Supplementary material related to this article can be found online at http://dx.doi.org.

REFERENCES

Amery, F., Degryse, F., Degeling, W., Smolders, E. and Merckx, R. (2007) The copper-mobilizing-potential of dissolved organic matter in soils varies 10-fold depending on soil incubation and extraction procedures. Environmental Science & Technology 41(7), 2277-2281.

Baken, S., Degryse, F., Verheyen, L., Merckx, R. and Smolders, E. (2011) Metal Complexation Properties of Freshwater Dissolved Organic Matter Are Explained by Its Aromaticity and by Anthropogenic Ligands. Environmental Science & Technology 45(7), 2584-2590.

Batchelli, S., Muller, F.L.L., Chang, K.C. and Lee, C.L. (2010) Evidence for Strong but Dynamic Iron-Humic Colloidal Associations in Humic-Rich Coastal Waters. Environmental Science & Technology 44(22), 8485-8490.

Berto, S., De Laurentiis, E., Tota, T., Chiavazza, E., Daniele, P.G., Minella, M., Isaia, M., Brigante, M. and Vione, D. (2016) Properties of the humic-like material arising from the photo-transformation of L-tyrosine. Science of the Total Environment 545-546, 434-444.

Boyle, E.S., Guerriero, N., Thiallet, A., Del Vecchio, R. and Blough, N.V. (2009) Optical Properties of Humic Substances and CDOM: Relation to Structure. Environmental Science & Technology 43(7), 2262-2268.

Brooks, M.L., McKnight, D.M. and Clements, W.H. (2007) Photochemical control of copper complexation by dissolved organic matter in Rocky Mountain streams, Colorado. Limnology and Oceanography 52(2), 766-779.

Buck, R.P., Singhadeja, S. and Rogers, L.B. (1954) Ultraviolet Absorption Spectra of Some Inorganic Ions in Aqueous Solutions. Analytical Chemistry 26(7), 1240-1242.

Bundy, R.M., Biller, D.V., Buck, K.N., Bruland, K.W. and Barbeau, K.A. (2014) Distinct pools of dissolved iron-binding ligands in the surface and benthic boundary layer of the California Current. Limnology and Oceanography 59(3), 769-787.

Chaminda, G.G.T., Nakajima, F., Furumai, H., Kasuga, I. and Kurisu, F. (2013) Metal (Zn, Cu, Cd and Ni) complexation by dissolved organic matter (DOM) in wastewater treatment plant effluent. Journal of Water and Environment Technology 11(3), 153-161.

Craven, A.M., Aiken, G.R. and Ryan, J.N. (2012) Copper(II) Binding by Dissolved Organic Matter: Importance of the Copper-to-Dissolved Organic Matter Ratio and Implications for the Biotic Ligand Model. Environmental Science & Technology 46(18), 9948-9955.

Croue, J.P., Benedetti, M.F., Violleau, D. and Leenheer, J.A. (2003) Characterization and copper binding of humic and nonhumic organic matter isolated from the South Platte River: Evidence for the presence of nitrogenous binding site. Environmental Science & Technology 37(2), 328-336.

Fimmen, R.L., Cory, R.M., Chin, Y.P., Trouts, T.D. and McKnight, D.M. (2007) Probing the oxidation-reduction properties of terrestrially and microbially derived dissolved organic matter. Geochimica Et Cosmochimica Acta 71(12), 3003-3015.

Frenkel, A.I., Korshin, G.V. and Ankudinov, A.L. (2000) XANES study of Cu^{2+}-binding sites in aquatic humic substances. Environmental Science & Technology 34(11), 2138-2142.

Fujii, M., Imaoka, A., Yoshimura, C. and Waite, T.D. (2014) Effects of Molecular Composition of

Natural Organic Matter on Ferric Iron Complexation at Circumneutral pH. Environmental Science & Technology 48(8), 4414-4424.

Gao, Y., Yan, M. and Korshin, G. (2015) Effects of calcium on the chromophores of dissolved organic matter and their interactions with copper. Water Research 81, 47-53.

Gilbert, B.; Ono, R. K.; Ching, K. A.; Kim, C. S., The effects of nanoparticle aggregation processes on aggregate structure and metal uptake. Journal of Colloid and Interface Science **2009,** 339(2), 285-295.

Hassler, C.S., Schoemann, V., Nichols, C.M., Butler, E.C.V. and Boyd, P.W. (2011) Saccharides enhance iron bioavailability to Southern Ocean phytoplankton. Proceedings of the National Academy of Sciences of the United States of America 108(3), 1076-1081.

Helms, J.R., Stubbins, A., Ritchie, J.D., Minor, E.C., Kieber, D.J. and Mopper, K. (2008) Absorption spectral slopes and slope ratios as indicators of molecular weight, source, and photobleaching of chromophoric dissolved organic matter. Limnology and Oceanography 53(3), 955-969.

Hertkorn, N., Benner, R., Frommberger, M., Schmitt-Kopplin, P., Witt, M., Kaiser, K., Kettrup, A. and Hedges, J.I. (2006) Characterization of a major refractory component of marine dissolved organic matter. Geochimica Et Cosmochimica Acta 70(12), 2990-3010.

Imai, A., Fukushima, T., Matsushige, K. and Kim, Y.H. (2001) Fractionation and characterization of dissolved organic matter in a shallow eutrophic lake, its inflowing rivers, and other organic matter sources. Water Research 35(17), 4019-4028.

Imai, A., Fukushima, T., Matsushige, K., Kim, Y.H. and Choi, K. (2002) Characterization of dissolved organic matter in effluents from wastewater treatment plants. Water Research 36(4), 859-870.

Karlsson, T. and Persson, P. (2010) Coordination chemistry and hydrolysis of Fe(III) in a peat humic acid studied by X-ray absorption spectroscopy. Geochimica Et Cosmochimica Acta 74(1), 30-40.

Karlsson, T., Persson, P. and Skyllberg, U. (2006) Complexation of copper(II) in organic soils and in dissolved organic matter - EXAFS evidence for chelate ring structures. Environmental Science & Technology 40(8), 2623-2628.

Karlsson, T. and Skyllberg, U. (2007) Complexation of zinc in organic soils - EXAFS evidence for sulfur associations. Environmental Science & Technology 41(1), 119-124.

Karthikeyan, K. G.; Elliott, H. A.; Chorover, J., Role of surface precipitation in copper sorption by the hydrous oxides of iron and aluminum. Journal of Colloid and Interface Science **1999,** 209(1), 72-78.

Keil, R.G. and Kirchman, D.L. (1991) Contribution of Dissolved Free Amino-Acids and Ammonium to the Nitrogen Requirements of Heterotrophic Bacterioplankton. Marine Ecology Progress Series 73(1), 1-10.

Laglera, L.M. and van den Berg, C.M.G. (2003) Copper complexation by thiol compounds in estuarine waters. Marine Chemistry 82(1-2), 71-89.

Laglera, L.M. and van den Berg, C.M.G. (2009) Evidence for geochemical control of iron by humic substances in seawater. Limnology and Oceanography 54(2), 610-619.

Louis, Y., Pernet-Coudrier, B. and Varrault, G. (2014) Implications of effluent organic matter and its hydrophilic fraction on zinc (II) complexation in rivers under strong urban pressure: Aromaticity as an inaccurate indicator of DOM-metal binding. Science of the Total Environment 490, 830-837.

Lu, Y.F. and Allen, H.E. (2001) Partitioning of copper onto suspended particulate matter in river waters. Science of the Total Environment 277(1-3), 119-132.

Matar, Z., Pereira, C.S., Chebbo, G., Uher, E., Troupel, M., Boudahmane, L., Saad, M., Gourlay-France, C., Rocher, V. and Varrault, G. (2015) Influence of effluent organic matter on copper speciation and bioavailability in rivers under strong urban pressure. Environmental Science and Pollution Research 22(24), 19461-19472.

McKnight, D.M., Boyer, E.W., Westerhoff, P.K., Doran, P.T., Kulbe, T. and Andersen, D.T. (2001) Spectrofluorometric characterization of dissolved organic matter for indication of precursor organic material and aromaticity. Limnology and Oceanography 46(1), 38-48.

Morris, D.P., Zagarese, H., Williamson, C.E., Balseiro, E.G., Hargreaves, B.R., Modenutti, B., Moeller, R. and Queimalinos, C. (1995) The attentuation of solar UV radiation in lakes and the role of dissolved organic carbon. Limnology and Oceanography 40(8), 1381-1391.

Nagao, S. (2008) Humic Substances in the Environment. Ishiwatari, R., Yonebayashi, K. and Miyajima, T. (eds), pp. 30-48, Sankyo Shuppan, Tokyo. (in Japanese)

Park, J.H., Lee, J.H., Kang, S.Y. and Kim, S.Y. (2007) Hydroclimatic controls on dissolved organic matter (DOM) characteristics and implications for trace metal transport in Hwangryong River Watershed, Korea, during a summer monsoon period. Hydrological Processes 21(22), 3025-3034.

Poulin, B.A., Ryan, J.N. and Aiken, G.R. (2014) Effects of iron on optical properties of dissolved organic matter. Environmental Science & Technology 48(17), 10098-10106.

Quinn, G.P. and Keough, M.J. (2002) Experimental Design and Data Analysis for Biologists Cambridge University Press, New York.

Ritchie, J.D. and Perdue, E.M. (2003) Proton-binding study of standard and reference fulvic acids, humic acids, and natural organic matter. Geochimica Et Cosmochimica Acta 67(1), 85-96.

Rozan, T.F., Lassman, M.E., Ridge, D.P. and Luther, G.W. (2000) Evidence for iron, copper and zinc complexation as multinuclear sulphide clusters in oxic rivers. Nature 406(6798), 879-882.

Shafer, M.M., Overdier, J.T., Hurley, J.P., Armstrong, D. and Webb, D. (1997) The influence of dissolved organic carbon, suspended particulates, and hydrology on the concentration, partitioning and variability of trace metals in two contrasting Wisconsin watersheds (USA). Chemical Geology 136(1-2), 71-97.

Smith, D.S., Bell, R.A. and Kramer, J.R. (2002) Metal speciation in natural waters with emphasis on reduced sulfur groups as strong metal binding sites. Comparative Biochemistry and Physiology C-Toxicology & Pharmacology 133(1-2), 65-74.

Spencer, R.G.M., Butler, K.D. and Aiken, G.R. (2012) Dissolved organic carbon and chromophoric dissolved organic matter properties of rivers in the USA. Journal of Geophysical Research-Biogeosciences 117, G03001.

Stolpe, B., Guo, L.D., Shiller, A.M. and Aiken, G.R. (2013) Abundance, size distributions and trace-element binding of organic and iron-rich nanocolloids in Alaskan rivers, as revealed by field-flow fractionation and ICP-MS. Geochimica Et Cosmochimica Acta 105, 221-239.

Tipping, E. (2002) Cation binding by humic substances, Cambridge University Press, UK.

Trivedi, P.; Dyer, J. A.; Sparks, D. L.; Pandya, K., Mechanistic and thermodynamic interpretations of zinc sorption onto ferrihydrite. Journal of Colloid and Interface Science **2004,** 270(1), 77-85.

Vachet, R.W. and Callaway, M.B. (2003) Characterization of Cu(II)-binding ligands from the Chesapeake Bay using high-performance size-exclusion chromatography and mass spectrometry. Marine Chemistry 82(1-2), 31-45.

van Den Berg, C.M.G., Merks, A.G.A. and Duursma, E.K. (1987) Organic complexation and its control of the dissolved concentrations of copper and zinc in the Scheldt Estuary. Estuarine Coastal and Shelf Science 24(6), 785-797.

Weishaar, J.L., Aiken, G.R., Bergamaschi, B.A., Fram, M.S., Fujii, R. and Mopper, K. (2003) Evaluation of specific ultraviolet absorbance as an indicator of the chemical composition and reactivity of dissolved organic carbon. Environmental Science & Technology 37(20), 4702-4708.

Wetzel, R.G. (1992) Gradient-Dominated Ecosystems - Sources and Regulatory Functions of

Dissolved Organic-Matter in Fresh-Water Ecosystems. Hydrobiologia 229, 181-198.

Yan, M. and Korshin, G.V. (2014) Comparative Examination of Effects of Binding of Different Metals on Chromophores of Dissolved Organic Matter. Environmental Science & Technology 48(6), 3177-3185.

Yan, M.Q., Benedetti, M.F. and Korshin, G.V. (2013a) Study of iron and aluminum binding to Suwannee River fulvic acid using absorbance and fluorescence spectroscopy: Comparison of data interpretation based on NICA-Donnan and Stockholm humic models. Water Research 47(14), 5439-5446.

Yan, M.Q., Dryer, D., Korshin, G.V. and Benedetti, M.F. (2013b) In situ study of binding of copper by fulvic acid: Comparison of differential absorbance data and model predictions. Water Research 47(2), 588-596.

Yan, M.Q., Lu, Y.J., Gao, Y., Benedetti, M.F. and Korshin, G.V. (2015) In-situ investigation of interactions between magnesium ion and natural organic matter. Environmental Science & Technology 49(14), 8323-8329.

Yan, M.Q., Wang, D.S., Korshin, G.V. and Benedetti, M.F. (2013c) Quantifying metal ions binding onto dissolved organic matter using log-transformed absorbance spectra. Water Research 47(7), 2603-2611.

Yang, L. and Hur, J. (2014) Critical evaluation of spectroscopic indices for organic matter source tracing via end member mixing analysis based on two contrasting sources. Water Research 59, 80-89.

Table 1. Summary of water quality parameters for waters from the Sagami River basin (SRB) and other natural freshwaters.[a]

(i) General

Water system	Climate	Section or water type	*n*	pH	Electrical conductivity (EC; mS.m^{-1})	Water temperature (T; °C)	Dissolved oxygen (DO; mM)	Chlorophyll-*a* (Chl-*a*) (µg.L^{-1})	Major cations (µM)[b]		Nutrients (µM)[b]				
									Ca	Mg	NO$_3$-N	NO$_2$-N	NH$_4$-N	PO$_4$-P	Si
SRB[c]	Temperate	Main stream	45-56	7.83 (6.40-9.42)	12.3 (8.89-16.7)	14.3 (6.0-25.1)	0.25 (0.19-0.38)	2.46 (0.0804-35.7)	384 (273-454)	195 (118-254)	62.8 (26.8-88.5)	0.521 (<0.357-2.28)	0.614 (<0.357-6.10)	0.439 (<0.161-2.84)	374 (221-535)
		Tributaries	17-27	7.85 (7.37-8.62)	7.62 (4.81-13.0)	13.3 (3.6-22.1)	0.25 (0.22-0.32)	0.747 (0.0245-3.45)	277 (228-358)	107 (82.8-143)	38.2 (23.8-73.1)	0.259 (<0.357-1.14)	0.813 (<0.357-4.68)	<0.161	264 (186-322)
		Reservoirs	10-14	7.98 (7.14-9.12)	11.8 (9.60-16.3)	15.2 (5.8-24.5)	0.26 (0.20-0.35)	10.0 (0.153-43.3)	357 (249-399)	187 (107-222)	55.0 (36.4-76.4)	0.910 (<0.357-2.57)	1.18 (<0.357-7.39)	0.281 (<0.161-1.42)	389 (240-478)
		WWTP effluents	8-12	6.79 (6.57-7.28)	52.7 (34.2-71.4)	21.6 (15.0-27.5)	0.17 (0.11-0.21)	(n.m.)	612 (484-705)	264 (189-349)	737 (493-1170)	8.92 (<0.357-21.4)	21.3 (<0.357-103)	37.9 (12.8-61.3)	406 (327-485)
Hwangryong River watershed, Korea (HRW)	Temperate	Headwater stream, river and reservoir	5	7.4 (7.1-7.7)	-	-	-	-	-	-	-	-	-	-	-
Yukon River basin, Alaska (YRB)	Subpolar	Spring flood	5	6.7 (6.0-7.6)	-	2.7 (0-6.6)	-	-	244 (110-390)	-	-	-	-	-	74 (51-92)
		Summer base flow	3	7.3 (7.1-7.5)	-	7.2 (5.1-9.3)	-	-	373 (340-390)	-	-	-	-	-	154 (139-180)
Freshwaters in Belgium and Germany (BGF)	Temperate	With few urban discharges upstream	12	-	-	-	-	-	-	-	-	-	-	-	-
		With urban discharges upstream	8												
		Acidic and Fe-rich water	3	-	-	-	-	-	-	-	-	-	-	-	-

[a] Mean value with range in parenthesis. Values below the detection limit were assumed as null when calculating the mean value. -: no data available. (n.m.): not measured.

[b] Total dissolved concentration.

[c] Full list of the water quality parameters measured for each sample is shown in SM Table S4.

Table 1. (Continued.)

(ii) Dissolved organic matter (DOM) properties and concentrations of total dissolved trace metals ($[\mathrm{Me}]_\mathrm{T}$)

Water system	Section or water type	Dissolved organic carbon ([DOC]; $\mathrm{mg.L^{-1}}$)	DOM optical indices[d]				$[\mathrm{Me}]_\mathrm{T}$ (nM)			Remarks	Reference
			A_{254} ($\mathrm{m^{-1}}$)[e]	$\mathrm{SUVA_{254}}$ ($\mathrm{L.mgC^{-1}.m^{-1}}$)[e]	$S_{275\text{-}295}$ ($\times 10^{-3}\ \mathrm{nm^{-1}}$)	FI	Cu	Fe	Zn		
SRB[c]	Main stream	1.15 (0.27-3.52)	2.21 (1.04-4.98)	2.36 (0.506-5.43)	16.5 (10.3-36.9)	1.80 (1.60-2.14)	15.2 (7.95-32.9)	69.1 (5.99-294)	23.8 (2.12-131)		This study
	Tributaries	0.700 (0.118-1.40)	1.27 (0.643-2.06)	1.71 (0.934-3.12)	16.7 (9.26-26.7)	1.74 (1.60-2.12)	6.70 (1.71-15.8)	54.8 (3.33-266)	12.5 (0.301-51.0)		
	Reservoirs	0.983 (0.360-1.66)	3.44 (2.07-5.91)	2.99 (1.64-4.39)	15.9 (13.5-19.4)	1.83 (1.68-2.01)	14.7 (9.13-24.8)	85.2 (<2.32-245)	14.9 (1.25-39.9)		
	WWTP effluents	5.15 (3.34-7.31)	10.6 (7.72-12.3)	2.13 (1.62-2.81)	10.8 (9.51-12.6)	2.18 (2.05-2.32)	56.2 (32.2-92.1)	419 (282-487)	629 (428-997)		
Hwangryong River watershed, Korea (HRW)	Headwater stream, river and reservoir	2.0 (1.1-2.9)	4.1 (1.9-7.1)	2.03 (1.41-2.46)	-	-	20.6 (17.8-23.4)	220 (72.7-455)	79.6 (53.4-121)		Park et al. (2007)
Yukon River basin, Alaska (YRB)	Spring flood	29.2 (9.37-56)	95.4 (34.1-158)	3.49 (2.83-4.17)	12.9 (12.2-13.4)	-	42 (33-62)	8,300 (2,400-15,000)	44 (17-101)	Influenced by permafrost.	Stolpe et al. (2013)
	Summer base flow	7.03 (4.32-11.5)	16.8 (7.56-30.8)	2.23 (1.75-2.68)	15.5 (13.8-17.1)	-	19 (14-26)	8,900 (2,900-17,000)	18 (15-21)		
Freshwaters in Belgium and Germany (BGF)	With few urban discharges upstream	5.9 (1.4-11.5)	14 (4.5-28)[f]	2.6 (1.4-3.6)	-	-	67 (26-130)[g]	-	35 (15-60)[g]	Stream, drainage ditch, reservoir and pond. APC 0.0-9.3 nM.[h]	Baken et al. (2011)
	With urban discharges upstream	3.8 (1.3-5.5)	8.8 (3.6-13)[f]	2.3 (1.8-2.8)	-	-	87 (25-160)[g]	-	94 (18-160)[g]	Stream. APC 4.8-139 nM.[h]	
	Acidic and Fe-rich water	38.7 (10.2-85.8)	170 (39-380)[f]	4.3 (3.8-4.6)	-	-	442 (109-978)[g]	>10,000	300 (58-690)[g]	Stream and marsh. APC 0.5-0.9 nM.[h]	

[d] See Supplementary Material (SM) Section S1 for the definition and characteristics of each index.

[e] Values for the SRB samples were corrected by using $[\mathrm{Fe}]_\mathrm{T}$ and nitrate concentration (when data were available). Values for HRW and YRB were corrected by using the reported $[\mathrm{Fe}]_\mathrm{T}$ as nitrate concentration was not available (see SM Section S3 for detail).

[f] Calculated from the reported values of [DOC] and $\mathrm{SUVA_{254}}$.

[g] Concentration of organically-complexed metal ([MeL]) calculated from the reported [DOC] and [MeL]/[DOC]. Note that [MeL] accounted for >99% and 83% on average of $[\mathrm{Cu}]_\mathrm{T}$ and $[\mathrm{Zn}]_\mathrm{T}$, respectively, in these samples (Baken et al., 2011).

[h] APC: aminopolycarboxylates (mainly ethylenediaminetetraacetic acid [EDTA]).

Table 2. Correlation coefficients between $[Me]_T$ and other water quality parameters in SRB.^{a}

	pH	EC (mS.m^{-1})	*T* (°C)	DO (mM)	Chl-*a* (μg.L^{-1})	Major cations (μM)		Nutrients (μM)					[DOC] (mg.L^{-1})	A_{254} (m^{-1})	SUVA$_{254}$ (L.mgC^{-1}.m^{-1})	$S_{275\text{-}295}$ (× 10^{-3} nm^{-1})	FI	$[Me]_T$ (nM)		
						Ca	Mg	NO_3-N	NO_2-N	NH_4-N	PO_4-P	Si						Cu	Fe	Zn
(i) Main stream (including the reservoirs [SGD and SYD]) (*n* = 26-69)																				
$[Cu]_T$	0.159	**0.299***	**0.400*****	-0.0339	***0.472******	**-0.305***	-0.210	0.0129	*0.216*	*-0.104*	**0.425***	-0.00520	**0.423*****	0.202	**-0.297***	*-0.209*	-0.221	-	-	-
$[Fe]_T$	*0.232*	*0.211*	***0.427******	*0.0385*	***0.539******	*-0.208*	*-0.164*	*-0.0778*	*0.189*	*0.0140*	0.326	*-0.141*	***0.398******	*0.215*	*-0.168*	***-0.268****	***-0.289****	***0.716******	-	-
$[Zn]_T$	*-0.146*	*-0.0305*	***-0.391******	*0.0400*	*-0.199*	***0.317*****	***0.349*****	***0.353*****	***-0.331****	*0.176*	*0.0664*	***0.256****	*-0.118*	-0.0678	0.153	*-0.195*	**0.368****	*0.146*	*-0.111*	-
(ii) Tributaries (*n* = 11-27)																				
$[Cu]_T$	0.0907	0.179	0.108	0.0725	0.314	0.263	0.228	0.246	*-0.156*	-0.192	(n.a.)	0.299	0.274	**0.502***	0.158	0.131	-0.0962	-	-	-
$[Fe]_T$	-0.155	-0.0732	0.106	-0.0283	0.111	-0.249	-0.299	-0.192	*-0.358*	-0.125	(n.a.)	0.0426	-0.00666	0.437	**0.489***	0.0419	-0.331	**0.623*****	-	-
$[Zn]_T$	0.0191	-0.264	-0.220	0.146	**0.568****	-0.0206	-0.0190	-0.0183	*0.179*	0.0265	(n.a.)	0.00963	-0.180	0.376	**0.517***	0.125	0.0157	0.221	0.0588	-
(iii) WWTP effluents (*n* = 7-11)																				
$[Cu]_T$	0.567	**-0.785***	**-0.714***	0.334	(n.a.)	-0.552	**-0.670***	**0.737****	0.0263	0.193	0.157	-0.0232	**-0.657***	-0.592	0.152	**-0.850****	0.510	-	-	-
$[Fe]_T$	0.104	0.196	0.379	0.0988	(n.a.)	-0.0511	-0.0918	0.0284	-0.472	-0.321	-0.201	0.00414	0.277	-0.543	0.323	-0.702	**0.790***	-0.140	-	-
$[Zn]_T$	-0.0910	-0.419	**-0.798****	0.0249	(n.a.)	0.226	-0.220	0.467	-0.337	0.191	0.345	-0.0174	-0.290	**-0.957*****	-0.211	-0.691	0.225	0.496	0.0592	-

^{a} Pearson's correlation coefficients were calculated when the normality of parameter set was confirmed; otherwise, Spearman's rank correlation coefficient was calculated and indicated in italic letters. The total number of data pair is shown as *n*. Bold-faced numbers indicate that the correlations are statistically significant (*: $p < 0.05$; **: $p < 0.01$; ***: $p < 0.001$). (n.a.): not applicable.

Table 3. Correlation coefficients between [Me]$_T$/[DOC] and other water quality parameters in SRB.[a]

	pH	EC (mS.m^{-1})	T (°C)	DO (mM)	Chl-a (μg.L^{-1})	Major cations (μM)		Nutrients (μM)					[Me]$_T$ (nM)			SUVA$_{254}$ (L.mgC^{-1}.m^{-1})	$S_{275\text{-}295}$ (× 10^{-3} nm^{-1})	FI
						Ca	Mg	NO$_3$-N	NO$_2$-N	NH$_4$-N	PO$_4$-P	Si	Cu	Fe	Zn			
(i) Main stream (including the reservoirs [SGD and SYD]) (n = 25-68)																		
[Cu]$_T$/[DOC]	-0.150	**-0.297***	**-0.372****	0.142	*-0.0789*	0.0809	0.214	-0.0538	*0.0339*	*0.322*	-0.0598	**0.366****	-	*0.0402*	***0.265****	**0.683*****	*0.115*	0.240
[Fe]$_T$/[DOC]	*0.0152*	*-0.0773*	*0.0347*	*0.164*	***0.274****	*-0.107*	*0.0394*	*-0.0906*	*0.0701*	*0.179*	*0.0169*	*-0.0107*	***0.359*****	-	*-0.0155*	***0.377*****	*-0.0241*	*-0.0843*
[Zn]$_T$/[DOC]	*-0.236*	***-0.334*****	***-0.704******	*0.205*	***-0.354*****	***0.390*****	***0.459******	*0.233*	***-0.357****	*0.351*	-0.144	***0.347*****	***-0.263****	***-0.317****	-	***0.511******	*0.0706*	***0.564******
(ii) Tributaries (n = 10-26)																		
[Cu]$_T$/[DOC]	**-0.516****	-0.375	**-0.432***	0.0772	-0.0937	-0.112	-0.153	-0.0768	*-0.172*	-0.235	(n.a.)	-0.0411	-	0.189	0.153	**0.688****	*-0.250*	-0.257
[Fe]$_T$/[DOC]	*-0.372*	*-0.224*	*-0.0903*	*-0.0739*	*0.112*	*-0.188*	*-0.273*	*-0.0605*	*-0.455*	-0.165	(n.a.)	*-0.0390*	*0.277*	-	*-0.119*	**0.718****	*-0.180*	*-0.393*
[Zn]$_T$/[DOC]	*-0.235*	***-0.555*****	***-0.611******	*0.311*	*-0.0168*	*-0.0855*	*-0.131*	*-0.122*	*0.216*	-0.142	(n.a.)	*-0.116*	*-0.0263*	*-0.0735*	-	**0.637****	*-0.0908*	0.00371
(iii) WWTP effluents (n = 6-9)																		
[Cu]$_T$/[DOC]	0.413	**-0.967*****	-0.566	0.616	(n.a.)	-0.363	**-0.916*****	0.480	-0.209	0.0577	0.264	-0.254	-	0.459	0.403	0.431	**-0.873****	0.664
[Fe]$_T$/[DOC]	0.109	**-0.860***	-0.287	0.444	(n.a.)	-0.0900	**-0.859****	0.0109	-0.134	-0.194	-0.0878	**-0.756***	0.583	-	0.335	0.614	-0.653	**0.783***
[Zn]$_T$/[DOC]	-0.0199	-0.753	**-0.738***	0.361	(n.a.)	0.277	-0.624	0.232	-0.436	0.0506	0.533	-0.356	0.510	0.369	-	0.153	**-0.715***	0.409

[a] Pearson's correlation coefficient was calculated when the normality of parameter set was confirmed; otherwise, Spearman's rank correlation coefficient was calculated and indicated in italic letters. The total number of data pair is shown as n. Bold-faced numbers indicate that the correlations are statistically significant (*: $p < 0.05$; **: $p < 0.01$; ***: $p < 0.001$). (n.a.): not applicable.

FIGURE CAPTIONS

Figure 1. The PCA results on the water quality variables for the SRB natural waters (panels (a) and (c)) and for all SRB waters (i.e., natural waters and WWTP effluents; panels (b) and (d)). Panels (a) and (b) indicate plots of the principal component (PC) loadings (first PC [PC1] versus second PC [PC2]) for the water quality variables as shown in the legend (top left). For the natural waters, PC1 and PC2 accounted for 26% and 20% of the total variance, respectively, whereas PC1 and PC2 explained 51% and 14% of the total variance, respectively, for all SRB waters. Panels (c) and (d) indicate plots of the PC scores (PC1 versus PC2) for the sampling stations and seasons are specified in SM Table S4. Symbols represent sampling seasons and water types as shown in the legend (top right).

Figure 2. The PCA results on the metal-to-DOC ratio (i.e., $[Me]_T/[DOC]$) and other water quality variables for the SRB natural waters (panels a and c) and all SRB waters (i.e., natural waters and WWTP effluents; panels b and d). Panels (a) and (b) indicate plot of the principal component (PC) loadings (PC1 versus PC2) for the parameters as shown in the legend (top left). For the natural waters, PC1 and PC2 explained 28% and 17% of the total variance, respectively. On the other hand, PC1 and PC2 accounted for 43% and 16% of the total variance, respectively, for all SRB waters. Panels (c) and (d) indicate plot of the PC scores (PC1 versus PC2) for sampling stations specified in SM Table S4. Symbols represent sampling seasons and water types as shown in the legend (top right).

Figure 3. Correlations between $SUVA_{254}$ and $[Me]_T/[DOC]$ for SRB natural waters (main stream [blue closed circles]: $n = 53$ for Fe and 55 for Cu and Zn; tributaries [green open circles]: $n = 17$) and effluent waters [pink closed circles]; $n = 7$ for Fe and 8 for Cu and Zn): (a) Cu, (b) Fe, and (c) Zn. Data from HRW and YRB natural waters were also plotted (Table 1; HRW [open diamond]: $n = 5$; YRB in spring [open triangle]: $n = 5$; YRB in summer [closed triangle]: $n = 3$) (Park et al. 2007; Stolpe et al., 2013). Data for YRB waters in summer were not shown in panel b because the values of $[Fe]_T/[DOC]$ for these waters were significantly higher than those for the other systems. (Data of $SUVA_{254}$ and $[Fe]_T/[DOC]$ for all the freshwater systems examined, including YRB in summer, are shown in Figure S6.) In addition, the BGF data ($SUVA_{254}$ and [MeL]/[DOC]) were plotted for Cu and Zn (Table 1; $n = 12$ for the waters without urban discharges [UD] upstream [open squares], 8 for those affected by UD [grey closed squares] and 4 for acidic Fe-rich waters [black closed squares]; error bars representing standard deviation). In BGF waters, fraction of DOM-metal complex accounted for a majority of total dissolved metal (e.g., >99% and 83% for Cu and Zn, respectively) (Baken et al. 2011). Blue solid, green dashed and black solid lines indicate the linear regression lines for the SRB main stream, SRB tributaries and BGF without UD, respectively. For these waters, significant linear correlations between $SUVA_{254}$ and $[Me]_T/[DOC]$ ($p < 0.01$) were found.

Figure 1

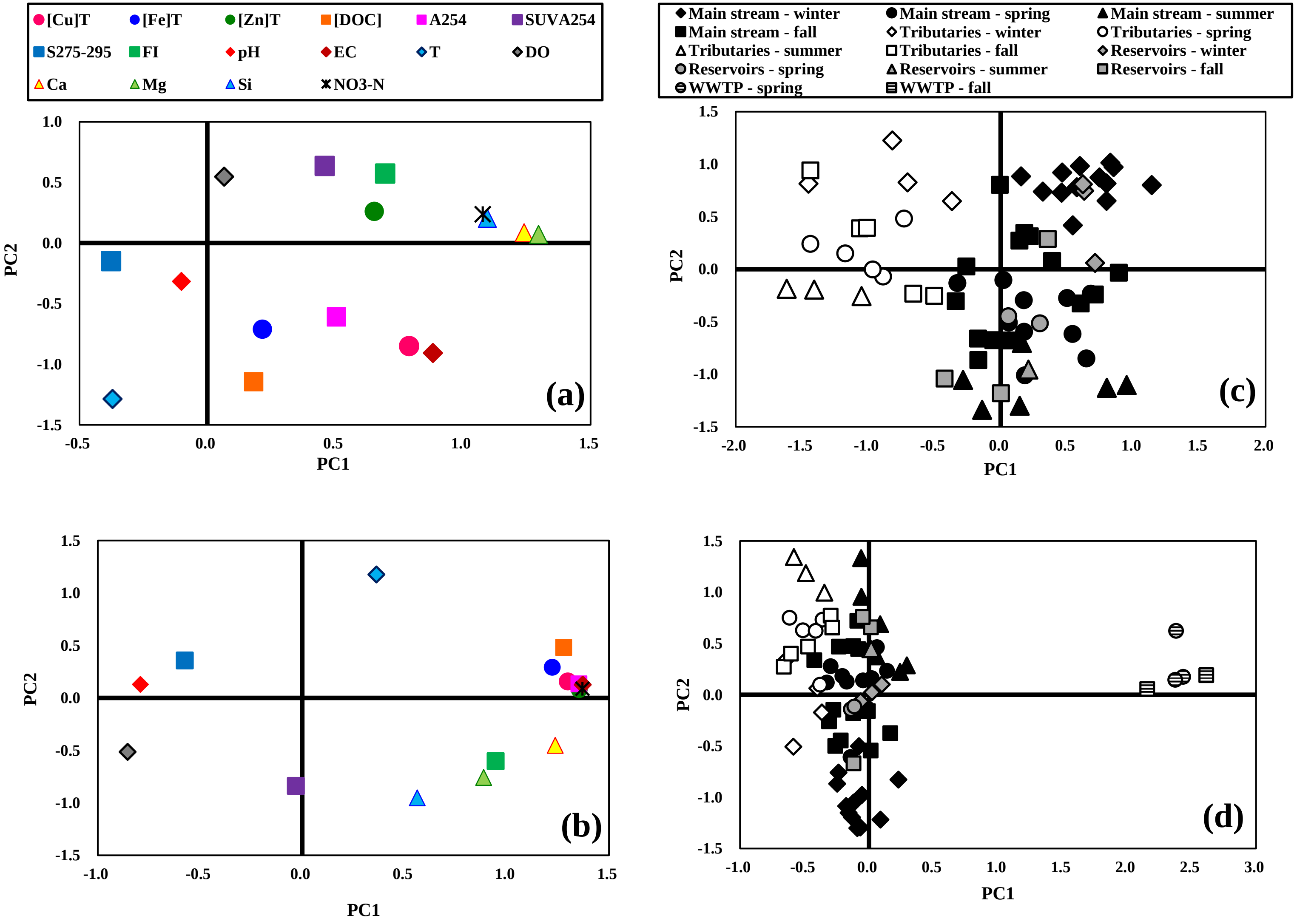
[Cu]T
[Fe]T
[Zn]T
[DOC]
A254
SUVA254
S275-295
FI
pH
EC
T
DO
Ca
Mg
Si
NO3-N
Main stream - winter
Main stream - spring
Main stream - summer
Main stream - fall
Tributaries - winter
Tributaries - spring
Tributaries - summer
Tributaries - fall
Reservoirs - winter
Reservoirs - spring
Reservoirs - summer
Reservoirs - fall
WWTP - spring
WWTP - fall
(a)
(b)
(c)
(d)
PC1
PC2
1.0
0.5
0.0
-0.5
-1.0
-1.5
1.5
2.0
2.5
3.0
-2.0

Figure 2

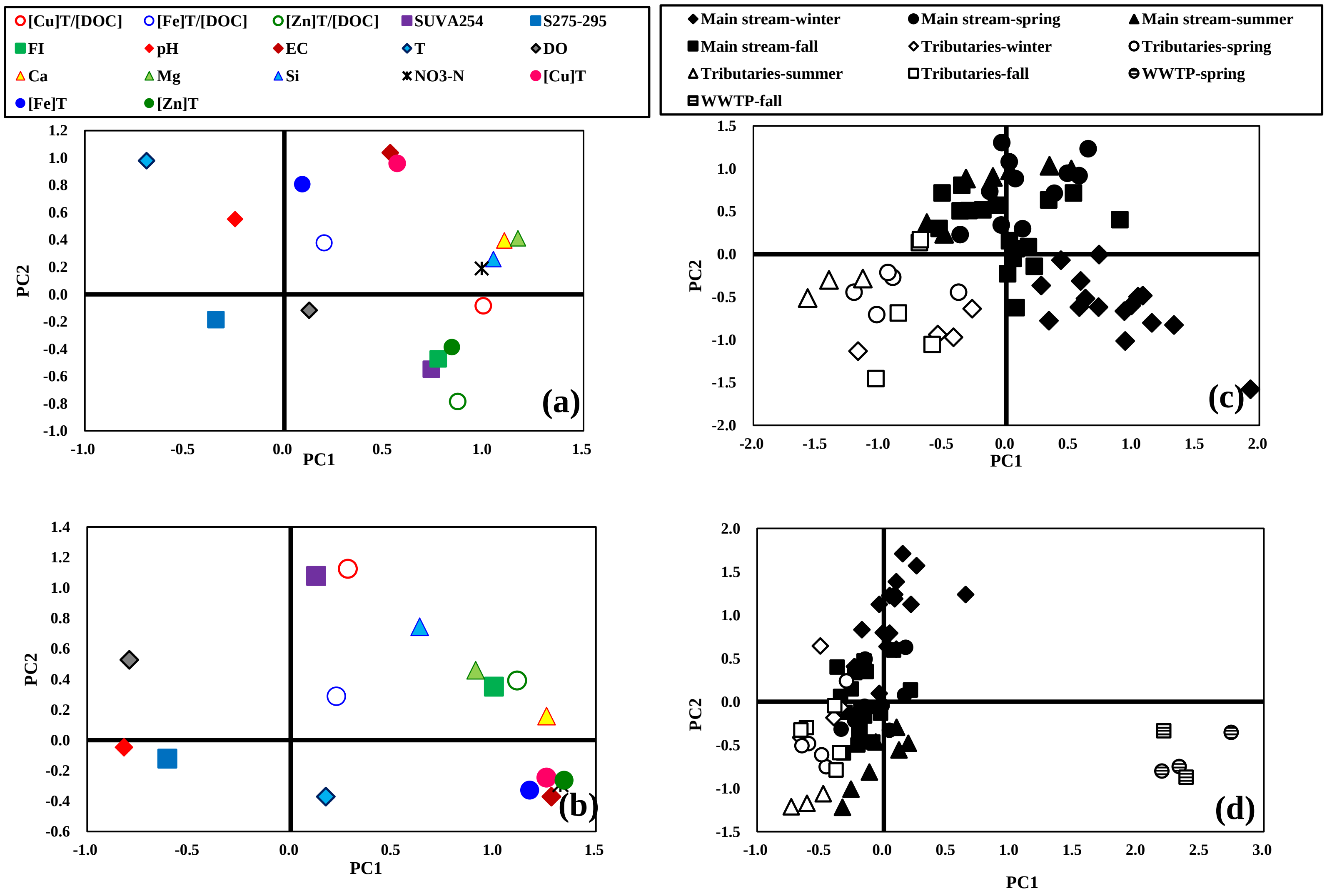

○[Cu]T/[DOC]
○[Fe]T/[DOC]
○[Zn]T/[DOC]
■SUVA254
■S275-295
■FI
◆pH
◆EC
◆T
◇DO
△Ca
△Mg
△Si
✱NO3-N
●[Cu]T
●[Fe]T
●[Zn]T
◆Main stream-winter
●Main stream-spring
▲Main stream-summer
■Main stream-fall
◇Tributaries-winter
○Tributaries-spring
△Tributaries-summer
□Tributaries-fall
⊖WWTP-spring
⊟WWTP-fall
(a)
(b)
(c)
(d)
PC1
PC2
1.4
1.2
1.0
0.8
0.6
0.4
0.2
0.0
-0.2
-0.4
-0.6
-0.8
-1.0
-1.5
-2.0
1.5
2.0
-1.0
-0.5
0.0
0.5
1.0
1.5
2.0
2.5
3.0

Figure 3

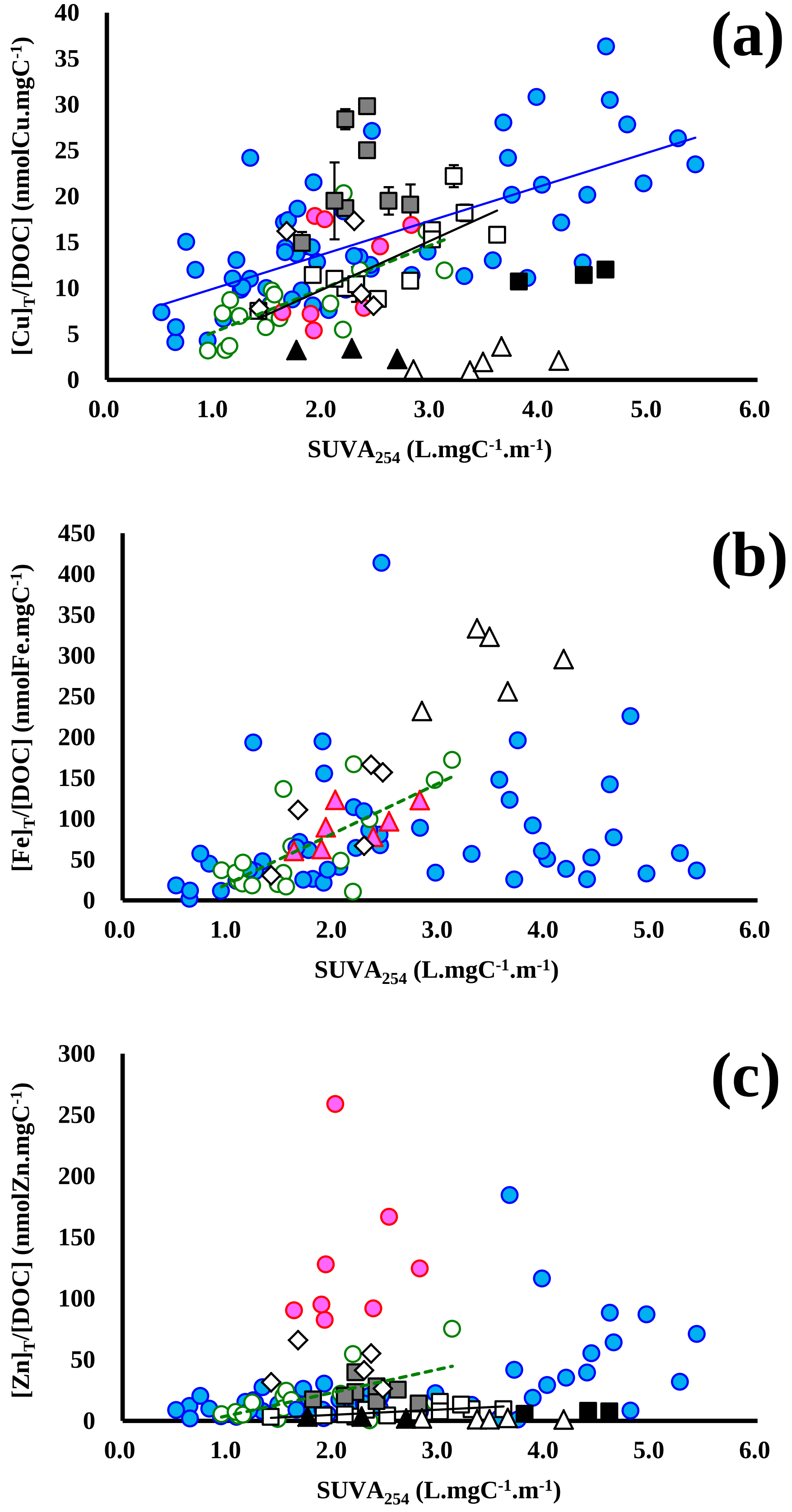
(a)
[Cu]T/[DOC] (nmolCu.mgC-1)
0
5
10
15
20
25
30
35
40
SUVA254 (L.mgC-1.m-1)
0.0
1.0
2.0
3.0
4.0
5.0
6.0
(b)
[Fe]T/[DOC] (nmolFe.mgC-1)
0
50
100
150
200
250
300
350
400
450
SUVA254 (L.mgC-1.m-1)
0.0
1.0
2.0
3.0
4.0
5.0
6.0
(c)
[Zn]T/[DOC] (nmolZn.mgC-1)
0
50
100
150
200
250
300
SUVA254 (L.mgC-1.m-1)
0.0
1.0
2.0
3.0
4.0
5.0
6.0